THE JOURNAL OF PHYSICAL CHEMISTRY B LETTERS

2005, *109,* 13043−13048
Published on Web 06/18/2005

Competing Thermal Activation Mechanisms in the Meltinglike Transition of Na_N ($N = 135-147$) Clusters

Andrés Aguado*

Departamento de Física Teórica, Universidad de Valladolid, Valladolid 47011, Spain

Received: April 9, 2005; In Final Form: June 2, 2005

The meltinglike transition in unsupported icosahedral Na_N clusters, with $N = 135-147$, has been studied by isokinetic molecular dynamics simulations based on an orbital-free version of density functional theory. A maximum in the melting temperature, T_m, is obtained for Na_{141}, while the latent heat, ΔE, and entropy of melting, ΔS, are maximal for Na_{147}. These observations are in close agreement with calorimetric experiments on Na_N^+ clusters. The size evolution of ΔS is rationalized by the emergence of important premelting effects associated with the diffusive motion of atomic vacancies at the cluster surface. The precise location of the maximum in T_m is explained in terms of two different thermally activated structural instability mechanisms which trigger the meltinglike transition in the size ranges $N = 135-141$ and $N = 141-147$, respectively.

The melting point, T_m, of a finite atomic system is expected to decrease from its corresponding bulk limit as the number of atoms, N, is reduced, because of the increased surface-to-volume ratio. This is indeed the observed behavior at the mesoscale level. At the nanoscale level, however, clusters formed by a few hundred or less atoms show important deviations from such a classical law. Jarrold and co-workers[1] have demonstrated that small gallium and tin clusters melt at temperatures higher than T_m^{bulk}. Also, calorimetry experiments by Haberland and co-workers[2,3] show that the size dependence of T_m is not monotonic for Na_N^+ clusters in the size range $N \approx 50-350$. In the first set of calorimetric experiments,[2] where only a reduced size range was covered, maxima in the $T_m(N)$ curve were associated with joint electronic and structural enhanced stability. For example, a local maximum in T_m was observed for Na_{142}^+ and a conjecture was made that the close proximity of both geometrical (Na_{147}^+) and electronic (Na_{139}^+) shell closings produced that maximum. However, later experiments in a wider size range[3] confirmed that T_m maxima are not correlated in general with known either electronic or geometrical shell closings. A very recent conjoint analysis of calorimetry experiments and photoelectron spectra[4] has demonstrated that maxima in the latent heat, ΔE, and entropy of melting, ΔS, are indeed correlated with *geometrical* shell closings, which demonstrate that electronic effects do not play an important role in the melting of sodium clusters with more than 50 atoms. Despite many theoretical efforts,[5−12] no definite explanation for the calorimetry experiments has emerged yet. Specifically, the experimental observations in the size range $N = 135-147$ still await a theoretical explanation and/or confirmation. In this letter, I show that molecular dynamics (MD) simulations, with an accurate (first-principles) representation of interatomic forces, reproduce the main trends of the calorimetry experiments in this size range.

This study has been performed using the orbital-free ab initio molecular dynamics (OF-AIMD) method, where the forces acting on the nuclei are computed from the electronic structure evaluated within density functional theory (DFT).[13] The interactions between atoms depend on the electronic structure. This is very important for a correct description of a metal cluster, as the nature of the interactions changes with coordination number, and therefore, it is crucial that the forces on atoms react to the electronic density distribution in their vicinity. In OF-AIMD, this is achieved by using an explicit but approximate density functional for the electron kinetic energy, which leads to a substantial simplification over the Kohn−Sham method of DFT.[14] The OF-AIMD method thus makes possible the simulation of large samples for long times.

The total potential energy of the system is written as the sum of the direct ion−ion Coulombic interaction energy and the ground state energy of the valence electron system. According to DFT, the ground state valence electron density, $\rho_g(\vec{r})$, minimizes an energy functional which is the sum of the kinetic energy of independent electrons, $T_s[\rho]$, the classical Hartree electrostatic energy, $E_H[\rho]$, the exchange-correlation energy, $E_{xc}[\rho]$, for which the local density approximation[15,16] is adopted, and the electron−ion interaction energy, for which analytical local pseudopotentials developed by Fiolhais et al.[17] are employed. In this work, the $T_s[\rho]$ functional is given by[18,19]

$$T_s[\rho] = T_{vW}[\rho] + T_\beta[\rho] \tag{1}$$

$$T_\beta = \frac{3}{10}\int d\vec{r}\ \rho(\vec{r})^{5/3-2\beta}\,\tilde{k}(\vec{r})^2 \tag{2}$$

$$\tilde{k}(\vec{r}) = (2k_F^0)^3 \int d\vec{s}\ k(\vec{s})\, w_\beta(2k_F^0|\vec{r} - \vec{s}|) \tag{3}$$

where $T_{vW} = (1/8)\int d\vec{r}(|\nabla\rho|^2/n)$ is the von Weizsäcker functional, $k(\vec{r}) = (3\pi^2)^{1/3}\rho(\vec{r})^\beta$, k_F^0 is the Fermi wave vector corresponding to a mean electron density, ρ_0, $\beta = 0.51$, and $w_\beta(x)$ is a weight

* E-mail: aguado@metodos.fam.cie.uva.es.

10.1021/jp051842t CCC: $30.25

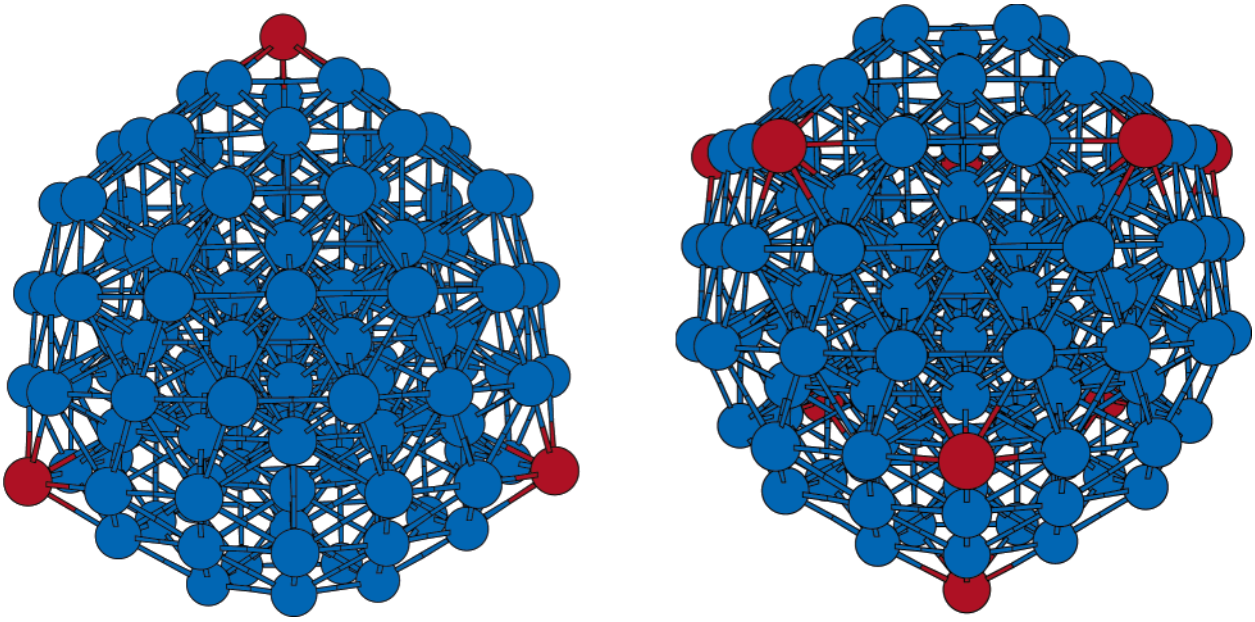

Figure 1. OF-AIMD ground state icosahedral isomers of Na_{138} and Na_{144}. Atoms at surface vertex positions are represented by red spheres and the rest of the atoms by blue spheres.

function, determined by requiring $T_s[\rho]$ to recover the correct expression for both the uniform density and linear-response-theory limits. The mean electron density is defined as $\rho_0 = V/N$, where V is the volume of a sphere with a radius equal to the mean gyration radius of the cluster. The parameters defining the Fiolhais pseudopotential[17] are obtained by requiring the OF-AIMD method to reproduce Kohn-Sham ab initio molecular dynamics (KS-AIMD) results for the interatomic forces and relative energies of selected cluster configurations, as explained elsewhere.[20] OF-AIMD reproduces KS-AIMD interatomic forces for sodium clusters in this size range to within 5% and energy differences between isomers to within 2%. Further details may be found in refs 18−20. I note here that the employed $T_s[\rho]$ functional provides an accurate description of several static and dynamic properties of bulk alkalis,[21] alkali surfaces,[22] and alkali clusters[20] and that it represents a substantial improvement over the semiclassical $T_s[\rho]$ expressions employed in our previous simulations of cluster melting.[7,18]

The photoelectron spectra measured by Haberland et al.[4] corroborate that icosahedral symmetry dominates the structure of cold Na_N^- clusters in the size range covered by the present study. Therefore, I assume that Na_N clusters, with $N = 135-147$, have icosahedral symmetry. Each cluster is placed in a unit cell of a cubic superlattice of length $L = 33$ au. The set of plane waves periodic in that superlattice, up to an energy cutoff of 20 Ry, is used as a basis set to expand the valence electron density. Forces on atoms are calculated through the Hellmann−Feynmann theorem only after the ground state density has been found. For all sizes within this range, it is found that the least bound atom is at a surface vertex position. Therefore, to locate the ground state (GS) structure of Na_{141}, for example, I consider all geometrically inequivalent possibilities of removing six vertex atoms from a perfect three-shell Na_{147} icosahedron and find the optimal set of atomic coordinates by using a conjugate gradient routine. Some examples of GS structures obtained this way are shown in Figure 1. The structural trends may be summarized in the following terms: for $N = 142-145$, the surface vacancies created by the removal of vertexlike atoms tend to be as separated as possible; that is, they repel each other; for $N = 137-140$, it is the vertex atoms that repel each other. Nevertheless, the energy differences between isomers obtained this way are of the order of 0.1 meV/atom, which means they can be considered as degenerate isomers in a practical sense. That is, isomers with different distributions of vacancies in vertex positions will be present in the experiments. The thermal properties of the different isomers are not expected to be very different, due to the surface premelting effects discussed below. Thus, from now on, I only consider the GS isomers predicted by OF-AIMD.

For each cluster size, I have performed isokinetic MD runs, in which the average kinetic energy is kept constant by velocity rescaling. The time step employed is 3 fs, and the total simulation length for each size is 5 ns. Multiple histogram techniques[23] are employed in order to extract smooth caloric and specific heat curves from the isokinetic runs performed at a discrete set of temperatures. A representative example of caloric curves is given in Figure 2, while melting temperatures, T_m (read from the specific heat maxima), latent heats per particle, $q = \Delta E/N$ (estimated from the step height between liquid and solid branches of the caloric curve at $T = T_m$), and entropies of melting per particle, $\Delta s = \Delta S/N$ (obtained from Clapeyron's relation $T_m = q/\Delta s$), are given in Figure 3. There is a striking agreement with experimental observations;[4] namely, (1) q and Δs increase on average in the size range $N = 135-147$, and (2) a maximum in T_m is observed for $N = 141$ in OF-AIMD and for $N = 142$ in the experiment. The global trends are quantitatively reproduced, and this is what we are interested in. The agreement is not expected to be perfect because of the approximations in the T_s and E_{xc} energy functionals, possible inaccuracies in statistical sampling at the transition region, and the fact that experimental clusters are charged while simulated clusters are neutral. Another point of agreement is that there are no appreciable discontinuous signatures of premelting transitions in the caloric curves. For the smallest sizes, where premelting effects (see below) are most important, Figure 2 shows that there is a slight curvature of the caloric curve at temperatures lower than T_m but not a discontinuous change as expected from a first-order phase transition. Our results for Na_{142} are also in very reasonable agreement with a recent KS-AIMD simulation by Chacko et al.[12] which reports a melting point of

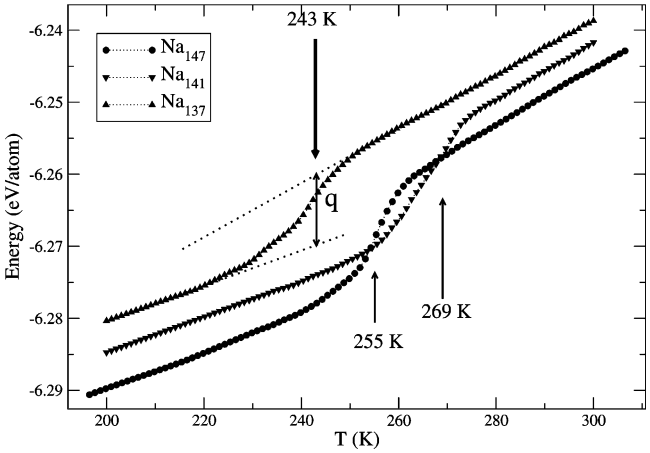

Figure 2. Representative sample of caloric curves obtained in this study. The arrows signal the corresponding melting temperatures at which the derivatives of the caloric curves (the specific heat per particle) attain a maximum value. The latent heat per particle, q, is obtained from the caloric curves by measuring the energy difference between liquid and solid branches at $T = T_m$, as shown for Na_{137}.

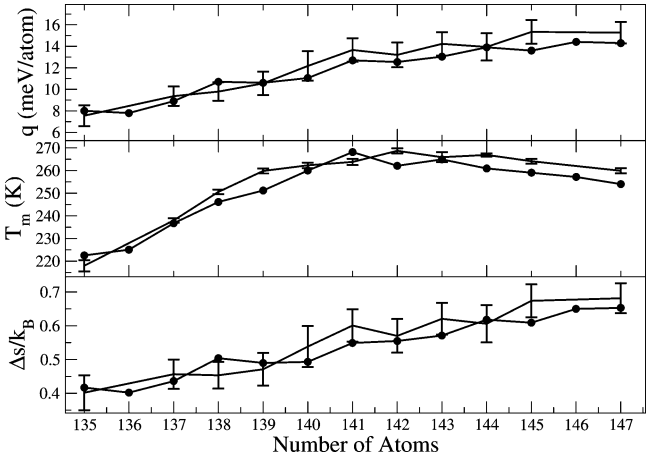

Figure 3. Size variation of the latent heat per atom (top), melting temperature (middle), and entropy of melting per atom (bottom) of Na_N ($N = 135-147$) clusters. The OF-AIMD results are indicated by full circles, and the error bars show the experimental results.[4]

290 K and a latent heat of 14.9 meV/atom, while the experimental values are between the OF-AIMD and KS-AIMD results.

The average size evolution of $q = [E_{liquid}(T_m) - E_{solid}(T_m)]/N$ is easiest to rationalize. In fact, if we instead consider the quantity $q_0 = [E_{liquid}(T_m) - E_{solid}(0\ K)]/N$ (not explicitly shown), it already displays the same average behavior. This means that the binding energy decrease upon removal of an atom is smaller in the liquid than in the solid phase; that is, it costs less energy to evaporate an atom in a liquid cluster within the size range considered. This is expected, as all atoms are tightly bound (highly coordinated) in the geometrically compact icosahedra considered here. This might not be the case if the solid phase contains, for example, floater atoms, that is, atoms outside a complete atomic shell, with a low coordination number. Oscillations of q about this average monotonic behavior, which are observed in both the experimental and OF-AIMD results, are small in magnitude and more difficult to rationalize. I have evaluated the evaporation energies at zero temperature, $E_{evap}(N) = E(1) + E(N-1) - E(N)$, and observed that local deviations in q from its average size dependence are correlated with $E_{evap}(N)$ (see Figure 4). I stress here that the energy

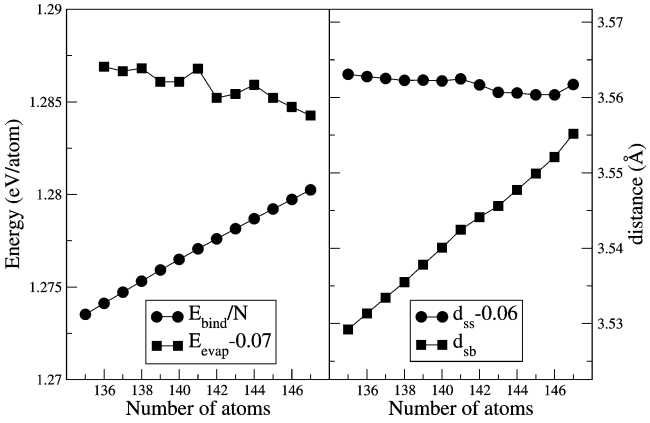

Figure 4. Size dependence of E_{bind}/N and E_{evap} (left) and of d_{ss} and d_{sb} (right). In both sides, one of the quantities has been displaced along the vertical axis to aid in visualization.

differences between different icosahedral isomers are so small that they do not affect the results of Figure 4. No matter which allocation of vertex atoms is chosen, it costs more energy to evaporate an atom from Na_{141} than from Na_{142}, for example. Thus, deviations from strictly monotonic behavior in $q(N)$ can be safely traced back to the size dependence of E_{evap} in (that is, relative stability of) the solid phase, but no simple explanation can be found for the size dependence of E_{evap} itself.

The entropy per atom of a liquid cluster can be safely assumed to be approximately size-independent,[4] at least within a narrow size range such as that considered here. Therefore, the size evolution of Δs must be explained in terms of the entropy per particle of the solid-phase clusters, for temperatures close to T_m. Our simulations predict (see below) that premelting effects are negligible for Na_{147}. However, important surface premelting effects are observed for $N = 135-146$, which are associated with the diffusive motion of atomic vacancies at the surface. Specifically, two different premelting mechanisms have been observed. The first mechanism is isomerizations where an atomic vacancy at a surface vertex site moves to a different surface vertex site. This mechanism, which is dominant in the size range $N = 142-146$, is illustrated in Figure 5: three surface atoms conjointly move along an icosahedral edge so that the vacancy can jump between two different vertex sites directly. A similar mechanism has been observed by Shimizu et al.[24] in simulations of the rapid alloying process in two-dimensional bimetallic clusters, and it is named the edge-running mechanism. Here, we show that the same mechanism is operative in realistic, three-dimensional clusters. The second mechanism is isomerizations where a surface atom moves from an edge to a hollow vertex position, so that the vacancy can explore also the edge sites at the surface. This mechanism is dominant for $N = 135-141$. I have never observed, within the length of the simulations, the vacancy to occupy a face position at the surface, which means that there are 20 surface atoms that do not displace during the premelting stage. From all of the surface atoms, facelike atoms have the largest coordination, so creation of a vacancy at a face position costs more energy. If we take into account the fact that face, edge, and vertexlike atoms at the surface shell have different radial distances (that is, the surface shell is formed by three different radial subshells), excitation of an edge atom to a hollow vertex site can be viewed as temporary thermal generation of a floater atom,[25] which is later neutralized by a neighboring surface vacancy. These premelting effects produce an increase in the entropy per atom of the solid phase before the cluster melts and provide an explanation for the size

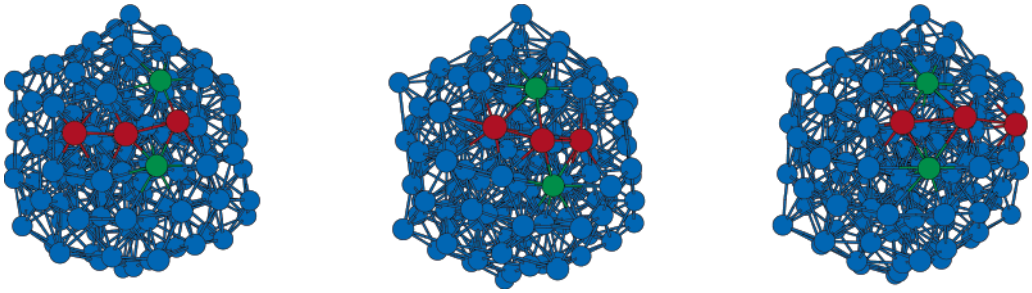

Figure 5. Snapshots taken from an OF-AIMD run on Na_{145}, showing the edge-running premelting mechanism. The surface vacancy can jump directly between two different vertex sites due to the cooperative displacement of a whole edge of atoms (marked in red). The other two atoms are shown in green in order to better appreciate the mechanism.

evolution of Δs. They also support the entropy model advanced by Haberland et al.[4] (which is indeed based on assuming mobility of surface atoms at temperatures lower than T_m), at least for those sizes immediately smaller than a geometrical shell closing. The premelting effects start approximately 20 K below T_m for Na_{146}, while for Na_{135} they start at temperatures as low as 100 K, more than 50% below T_m!

Figure 3 shows that the present simulations reproduce the experimental observation that q and Δs are highly correlated in their size dependence. Δs is larger the higher the structural order of the solid phase just before melting and therefore attains a maximum at $N = 147$. The fact that q is maximum at exactly the same size provides direct experimental evidence that electronic shell closing effects are at most of secondary importance to the cluster melting phenomenon. Otherwise, we would expect q to be maximum at a different size, closer to the electronic shell closing at $N = 138$. As the number of electrons does not change upon melting, this observation is not so strange. In any case, this is one important reason OF-AIMD studies, which do not reproduce electronic shell closing effects,[7,18,20] may give accurate predictions about the melting of unsupported Na clusters.

It should be stressed here that, although the premelting effects observed will result in surface diffusion in the long run, they are not characteristic of a surface melting stage (namely, a liquid layer on top of a solid core shell). The structural surface disorder is never high, as only a well-defined number of icosahedral isomers are visited during the premelting stage, which should be best described as a highly concerted isomerization stage. In fact, this is the reason premelting does not lead to any marked feature in the caloric curve: the isomers visited have a substantially lower energy than those corresponding to a fully disordered surface.

It has been pointed out by Haberland et al.[4] that the size evolutions of q and Δs show a high correlation with geometric shell closings, while the melting temperatures themselves show just a partial correlation. Also, Clapeyron's equation tells us that knowledge of q and Δs suffices to determine T_m. Therefore, q and Δs are apparently more basic quantities than T_m to explain the irregular size dependence of the meltinglike transition. However, the intensive variable (in this case T) is the one directly controlled in the experiments and present OF-AIMD simulations. Moreover, Clapeyron's relation describes just the thermodynamics of melting, but the meltinglike transition is a dynamic phenomenon, which must be initiated by a well-defined structural instability in the solid-phase cluster. This instability acts as a seed that triggers the development of the liquid phase. Thus, Clapeyron's equation alone does not provide any physical insight as to why the maximum in T_m is located at $N = 141$. Let me elaborate this point in detail: with decreasing size starting from $N = 147$, the decrease of Δs is initially more marked than that of q, which results in an increase of the melting temperature, T_m. In the size range $N = 135-141$, however, the rate of change of q is larger than that of Δs, which results in a T_m maximum at $N = 141$. Why do the rates of change of q and Δs evolve with size in such a way that their ratio is a maximum at $N = 141$? It is important to notice that the value of Δs is not very sensitive to the precise location of the melting point, as the entropy of the solid phase increases for temperatures considerably lower than T_m. On the contrary, as the liquid and solid branches of the caloric curves have different slopes, q is much affected by a change in melting point. That is, if T_m was reduced by, for example, 10 K, satisfaction of Clapeyron's equation would imply that the change in q would be much larger than the change in Δs. Δs is therefore a more stable quantity than q. In what follows, I suggest that identification of the structural instability mechanism may provide a more satisfying explanation for the size dependence of T_m than direct interpretation of the size evolution of q. The viewpoint adopted here is that the structural instability occurs at a given critical temperature, which is therefore the basic variable, while the latent heat, q, is considered a *consequence* of the melting transition.

Irrespective of the premelting effects discussed above, the structural instability mechanism which triggers the melting transition is observed to be the same in the size range $N = 141-147$ and involves the conjoint thermal excitation of surface atoms. Just below T_m, the surface of the cluster is very fluxional, with surface atoms undergoing very large amplitude vibrations. The displacements of atoms are highly concerted, in both the tangential and radial directions: when the instantaneous radial position of a surface atom is displaced inward, those nearest atoms in the radial shell immediately below expand in the tangential direction, and vice versa. Also, a set of neighboring atoms at the surface shell has instantaneously short interatomic distances only when their radial positions increase, and vice versa. At $T = T_m$, a critical stage is achieved when the distance between two neighboring surface atoms is temporarily so large that a neighboring third surface atom may move across the space left by the bond expansion. The net result is that the identity of vertex, edge, and facelike atoms at the surface is interchanged. The whole process involves the concerted rearrangement of the positions of many surface atoms (as opposed to the surface vacancy migration outlined above) and propagates to involve the whole cluster surface very fast, which results in a disordered surface structure. Once the surface disorder is initiated, it acts as a catalyst of homogeneous melting, which occurs at the same temperature. Shimizu et al.[24] have also observed that surface disorder may lead to radial diffusion in 2D metal clusters. Our OF-AIMD simulations thus do not predict a separate surface

melting stage, although surface diffusion is present at $T < T_m$ for $N < 147$ through the premelting mechanisms discussed above.

Figure 4 shows that evaporation energies are always larger than the corresponding binding energies per atom, implying that surface atoms have a higher stability than an average atom, in energetic terms. This may be the reason homogeneous melting sets in as soon as the surface melts. It also shows that the relative stability of surface atoms increases from $N = 147$ to $N = 135$. This can be traced back to the radial distance, d_{sb}, separating the surface atomic shell from the shell immediately below. This distance decreases with N by close to 1% within the size range considered here, while the average distance between surface atoms, d_{ss}, changes by less than 0.1%, which stabilizes surface atoms. Although barriers against evaporation are not necessarily correlated with barriers against diffusion, the results of Figure 4 are at least indicative that it costs more energy to break bonds at the cluster surface the smaller the size of the cluster. Thus, a higher temperature is needed to activate the structural instability when passing from $N = 147$ to $N = 141$.

Figure 4 thus shows that there exists a correlation between the melting points in the size range $N = 141-147$ and the distribution of potential energy into core and surface regions. Although such a correlation is very appealing because of its conceptual simplicity,[9] Calvo et al.[26] have provided counterexamples which demonstrate that it is by no means universal. In particular, it may be a consequence of nonergodic behavior in the MD simulations. Our OF-AIMD results predict that the liquid phase is directly accessed from the icosahedral isomer, which has the lowest energy at zero temperature. In contrast, a typical Monte Carlo simulation would include contributions to the thermodynamic functions from other sets of solidlike isomers (decahedral, bcc-like, etc.), each with its appropriate statistical (Maxwell−Boltzmann or Tsallis) weight, which would make the melting point depend on the *global* properties of the potential energy surface (PES). It is still an open question which of these scenarios is more appropriate to describe the experiments of Haberland's group, because there is no detailed information about the relative populations of isomers in the experimental beams as a function of temperature. Haberland and co-workers[4] report, however, that measured photoelectron spectra in this size range are best fitted by icosahedral structures, suggesting a very low population for isomers with other symmetries, at least at those temperatures where the spectra were measured. I have checked that the distribution of potential energy into core and surface regions is qualitatively the same for the family of decahedral isomers with $N = 135-147$, which would enlarge the limit of validity of the correlation for the case of Na clusters. In any case, this correlation, which considers just the *local* information about the PES provided by the icosahedral basin, is valid within our MD framework, which samples only the thermal instabilities of the icosahedral isomer.

If the structural instability mechanism which is a precursor of melting were the same in the whole range $N = 135-147$, we would expect an approximately monotonic increase of T_m with decreasing size, as the energy cost of breaking surface bonds continues to increase. OF-AIMD simulations predict, however, that the dynamical melting mechanism is different in the size range $N = 135-140$, providing a tentative explanation for the maximum in T_m. When the number of surface vacancies is considerable, wide amplitude concerted vibrations at the surface lead to the temporary creation of large "voids", which can be filled with an atom from the atomic shell immediately below. This process does not leave a vacancy in the interior of the cluster because a surface atom (specifically, I always observe it to be a facelike atom, which has the shortest radial distance) moves to the inner part almost at the same time. This means that radial diffusion is activated at a lower temperature than surface diffusion for these sizes; that is, interlayer mixing is easier than intralayer mixing. The process is again highly concerted, as the two atoms involved (one leaving and the other entering the surface shell) are always far apart. Homogeneous melting sets in directly in these clusters, apart from the premelting effects leading to the increase of the solid-phase entropy, discussed above. It is intuitively clear that interlayer mixing will be less impeded the larger the number of surface vacancies, which explains the trends observed in the size evolution of T_m. The picture that emerges from this study is that the decrease in T_m induces the large size dependence of the latent heat in this size range; that is, the energy of the liquid phase which is accessed at $T = T_m$ is lowered relative to that of the solid phase on account of the difference in heat capacities of the two phases (see Figure 2).

A realistic MD simulation of melting in small clusters requires both accurate interatomic forces and statistical sampling. Improved ergodicity is usually obtained by employing phenomenological parametrized descriptions of atomic interactions, at the cost of employing much less accurate interatomic forces. On the opposite side, KS-AIMD simulations provide accurate forces but it is presently difficult to routinely achieve ergodicity for clusters of this size. (Although Chacko et al.[12] have very recently demonstrated that well-converged KS-AIMD simulations of melting of Na_{142} are feasible, such calculations are by no means routine. Present OF-AIMD simulations, on the contrary, may run on a single Pentium processor routinely. Moreover, the computational expense of the calculations does not increase much when dealing with clusters of about 300 atoms,[20] as expected from a code which scales almost linearly with size. In this work, we have been able to simulate the meltinglike transition for 13 *different clusters* with about 140 particles, which enlarges by more than 1 order of magnitude the total simulation length covered by Chacko et al.) I would like to stress here that the present OF-AIMD results try to meet both accuracy criteria as close as possible. It has already been demonstrated that OF-AIMD forces closely match KS-AIMD forces for Na clusters of these sizes.[20] Now, the added computational simplicity (order-N scaling) of OF-AIMD simulations[7,18] can be exploited to simulate larger systems for longer times in a routine way, as compared to KS-AIMD. The present simulations are between 300 and 400 ps long at the transition region, which is a considerable time for a first-principles method, especially if we are considering 13 different sizes. It is true that much longer simulations are needed in order to observe some phenomena. For example, the possible dynamic coexistence of liquid and solid phases at a given temperature has to be studied with parametrized potentials. Also, quantities such as diffusion constants, D, or rms bond-length fluctuations, δ,[7] are possibly not fully converged by the present OF-AIMD simulations for those temperatures where the premelting effects are important (although they are well converged for fully solid or fully liquid phases). These structural quantities are converged only when the surface vacancies have explored all possible surface sites, which may take a long time at the premelting stage. The caloric curve, on the other hand, is not so sensitive to this complete exploration because the premelting mechanism samples many isomers which differ only in the permutation of atoms and thus have the same energy. I have checked that the caloric curves (the main results presented here) obtained by reducing

by 30% the simulation times are the same within roundoff errors. Full ergodicity is thus just a sufficient (as opposed to necessary) condition to obtain sufficiently accurate melting points. The present OF-AIMD simulations thus provide accurate forces, which is *essential* for a realistic simulation that can be meaningfully compared to experiment, and make an important effort in obtaining a reasonable statistical sampling.

In summary, I have reported first-principles MD simulations that reproduce and explain for the first time the main trends observed in the calorimetric experiments[4] in the size range $N = 135-147$. The size evolutions of the latent heat and entropy of melting are found to be maximal for $N = 147$, which means they are correlated with geometric shell closings. It has been stressed this observation implies that electronic shell closing effects can only be of secondary importance to the melting process, at least within the size range considered in this work, which makes the OF-AIMD method suitable to address the melting problem in sodium clusters. Important premelting effects, associated with the diffusion of atomic vacancies at the surface, are observed at temperatures below T_m for all sizes except Na_{147}, which explains the size evolution of the entropy of melting. To find an explanation for the maximum of T_m, observed for Na_{141}, the thermally induced structural instabilities leading to melting have been analyzed. It has been found that two different structural instabilities trigger melting in the size ranges $N = 135-141$ and $N = 141-147$. The size dependence of the activation energies for these mechanisms explain the size dependence of T_m. The fact that the OF-AIMD method reproduces experimental results with almost quantitative accuracy is probably somewhat fortuitous due to the several approximate functionals employed and possible inaccuracies in statistical sampling, but no much better agreement should be expected either from phenomenological potentials or presently affordable KS-AIMD simulations. It is the author's opinion that the emphasis of this work should be put instead on the correct reproduction of *experimental trends*.

Acknowledgment. This work was supported by DGES (project MAT2002-04393-C02-01) and the "Ramón y Cajal" program of the Spanish Ministry of Science and Technology.

References and Notes

(1) Shvartsburg, A. A.; Jarrold, M. F. *Phys. Rev. Lett.* **2000**, *85*, 2530. Breaux, G. A.; et al. *Phys. Rev. Lett.* **2003**, *91*, 215508; *J. Am. Chem. Soc.* **2004**, *126*, 8628.

(2) Schmidt, M.; et al. *Phys. Rev. Lett.* **1997**, *79*, 99; *Nature* **1998**, *393*, 238. Kusche, R.; et al. *Eur. Phys. J. D* **1999**, *9*, 1.

(3) Schmidt, M.; et al. *C. R. Phys.* **2002**, *3*, 327; *Phys. Rev. Lett.* **2003**, *90*, 103401.

(4) Haberland, H.; et al. *Phys. Rev. Lett.* **2005**, *94*, 035701.

(5) Blaise, P.; et al. *Phys. Rev. B* **1997**, *55*, 15856.

(6) Rytkönen, A.; et al. *Phys. Rev. Lett.* **1998**, *80*, 3940. Manninen, K.; et al. *Phys. Rev. A* **2004**, *70*, 023203.

(7) Aguado, A.; et al. *J. Chem. Phys.* **1999**, *111*, 6026; *J. Phys. Chem. B* **2001**, *105*, 2386; *Eur. Phys. J. D* **2001**, *15*, 221.

(8) Calvo, F.; Spiegelmann, F. *Phys. Rev. Lett.* **1999**, *82*, 2270; *J. Chem. Phys.* **2000**, *112*, 2888; **2004**, *120*, 9684.

(9) Lee, Y. J.; et al. *Phys. Rev. Lett.* **2001**, *86*, 999.

(10) Reyes-Nava, J. A.; et al. *Phys. Rev. B* **2003**, *67*, 165401.

(11) Manninen, K.; et al. *Eur. Phys. J. D* **2004**, *29*, 39.

(12) Chacko, S.; Kanhere, D. G.; Blundell, S. A. *Phys. Rev. B* **2005**, *71*, 155407.

(13) Hohenberg, P.; Kohn, W. *Phys. Rev.* **1964**, *136*, 864B.

(14) Kohn, W.; Sham, L. J. *Phys. Rev.* **1965**, *140*, 1133A.

(15) Perdew, J. P.; Zunger, A. *Phys. Rev. B* **1981**, *23*, 5048.

(16) Ceperley, D. M.; Alder, B. J. *Phys. Rev. Lett.* **1980**, *45*, 566.

(17) Fiolhais, C.; et al. *Phys. Rev. B* **1995**, *51*, 14001; **1996**, *53*, 13193.

(18) Aguado, A.; et al. In *Progress in Chemical Physics Research*; Columbus, F., Ed.; Nova Science Publishers: New York, in press.

(19) González, D. J.; et al. *Phys. Rev. B* **2002**, *65*, 184201.

(20) Aguado, A.; López, J. M. *Phys. Rev. Lett.* **2005**, *94*, 233401.

(21) González, D. J.; et al. *Phys. Rev. E* **2004**, *69*, 031205. Blanco, J.; et al. *Phys. Rev. E* **2003**, *67*, 041204.

(22) González, D. J.; et al. *Phys. Rev. Lett.* **2004**, *92*, 085501.

(23) Labastie, P.; Whetten, R. L. *Phys. Rev. Lett.* **1990**, *65*, 1567.

(24) Shimizu, Y.; Kobayashi, T.; Ikeda, S.; Sawada, S. *Adv. Chem. Phys.* **2005**, *130*, 155 and references therein.

(25) Cheng, H. P.; Berry, R. S. *Phys. Rev. A* **1992**, *45*, 7969.

(26) Calvo, F.; Doye, J. P. K.; Wales, D. J. *Phys. Rev. Lett.* **2001**, *87*, 119301.